Dalton Transactions

PAPER

View Article Online
View Journal | View Issue

Cite this: *Dalton Trans.*, 2016, **45**, 5038

A combined quantum-chemical and matrix-isolation study on molecular manganese fluorides†‡

Felix Brosi,[a] Tobias Schlöder,[a] Alexei Schmidt,[b] Helmut Beckers[a] and Sebastian Riedel*[a,b]

Received 10th December 2015,
Accepted 18th January 2016

DOI: 10.1039/c5dt04827c

www.rsc.org/dalton

Molecular manganese fluorides were studied using quantum-chemical calculations at DFT and CCSD(T) levels and experimentally by matrix-isolation techniques. They were prepared by co-deposition of IR-laser ablated elemental manganese or manganese trifluoride with F_2 in an excess of Ne, Ar, or N_2 or with neat F_2 at 5–12 K. New IR bands in the Mn–F stretching region are detected and assigned to matrix-isolated molecular MnF_x (x = 1–3).

Introduction

Manganese is an essential element for all living creatures and plays a key role in the process of photosynthesis.[1] Beyond that it has gained importance on a laboratory scale as a reagent for quantitative analysis[2] and on an industrial scale as an alloy component.[3] This is mostly due to its high bonding affinity towards oxygen that culminates in the stability of Mn_2O_7 [4] which contains manganese in its highest possible oxidation state +VII. For the stabilization of high positive oxidation states very electronegative ligands are necessary and besides oxygen also fluorine is used.[5] The highest oxidation state of a manganese fluoride is +IV in solid MnF_4.

In the binary system of manganese and fluorine MnF has gained attention due to the high multiplicity of its $^7\Sigma^+$ ground state. MnF has been studied extensively by theoretical methods[6] as well as experimentally using mass spectrometry,[7] rotational,[8–10] matrix-infrared[11] and electron spin resonance spectroscopy.[12] Commercially available MnF_2 and MnF_3 have been studied in detail in both solid and gaseous forms especially with regard to Jahn–Teller-distortion[12–14] using gas-phase electron diffraction,[15,16] X-ray diffraction,[17,18] neutron scattering,[19] vibrational spectroscopy,[20–22] and mass spectrometry.[7,23] MnF_2 and MnF_3 were thermally evaporated using a Knudsen cell and subsequently deposited in solid argon and neon matrices.[20,21] Another approach to study molecular MnF_x species is from thermally generated manganese atoms, which were treated with elemental fluorine. MnF, MnF_2 and MnF_3 were formed, and an IR band obtained in solid Ar at 768.7 cm^{-1} was tentatively assigned to "a molecule richer in fluorine than MnF_3".[11] MnF_4 is a blue solid, first synthesized in 1961[24] and later employed in the chemical synthesis of elemental fluorine.[25] It has been characterized in the solid state by X-ray diffraction,[26] vibrational spectroscopy[22,27] and magnetic susceptibility measurements.[24,28] Since it cannot be evaporated without decomposition to MnF_3 and F_2 [29] the investigation of molecular MnF_4 is challenging. In an earlier study solid MnF_3 was treated with TbF_4 at 700 K and an IR band at 794.5 cm^{-1} in the MnF stretching region as well as two weaker bands at 172.9 cm^{-1} and 176.6 cm^{-1} of the Ar-matrix isolated products were claimed to be molecular MnF_4.[23] From the appearance of a single band in the Mn–F stretching region a tetrahedral structure was deducted.

The fact that up to now binary fluorides of manganese higher than MnF_4 have not been obtained is remarkable. The heavier homologue technetium forms TcF_6,[30] while TcF_7 is predicted to be stable,[31] and ReF_7 is well-known.[32] FeF_4 and CrF_5 have been characterized,[33,34] while earlier reports on the existence of CrF_6 were shown to be erroneous.[35] A previous report about the possible existence of manganese pentafluoride taking into account thermochemical data and sterical considerations[36] stimulated us to reinvestigate the higher molecular Mn–F species using quantum-chemical calculations at DFT and CCSD(T) levels and to conduct matrix-isolation experiments in combination with IR spectroscopy.

Instead of thermally evaporating manganese, we have used the IR-laser ablation of elemental manganese to generate more reactive excited manganese atoms, which were co-condensed with fluorine diluted (0.25–3%) in neon, argon or nitrogen and neat fluorine. In addition we report about IR-laser ablation of manganese trifluoride, which has not been described previously.

[a]*Institut für Chemie und Biochemie - Anorganische Chemie, Freie Universität Berlin, Fabeckstraße 34/36, D-14195 Berlin, Germany. E-mail: s.riedel@fu-berlin.de*
[b]*Institut für Anorganische und Analytische Chemie, Albert-Ludwigs-Universität Freiburg, Albertstraße 21, D-79104 Freiburg i. Br., Germany*
† Dedicated to Prof. Dieter Lentz on the occasion of his 65th birthday.
‡ Electronic supplementary information (ESI) available. See DOI: 10.1039/c5dt04827c

Results and discussion

Calculated structures, thermochemistry and vibrational frequencies

Optimized structures for the binary manganese fluorides MnF_x (x = 1–7) are shown in Fig. 1.

The binary manganese fluorides have a high-spin ground state. The bond length of diatomic MnF calculated at the CCSD(T) level by Nhat *et al.* was 185 pm,[6] which is fairly close to our value of 184.3 pm at the DFT level and that obtained experimentally by rotational spectroscopy (183.9 pm).[10] MnF_2 is computed to be linear with a CCSD(T) bond length of 181.6 pm. Gas phase electron diffraction gave a consistent value of 181.1 pm.[15] MnF_3 has a distorted trigonal planar structure.

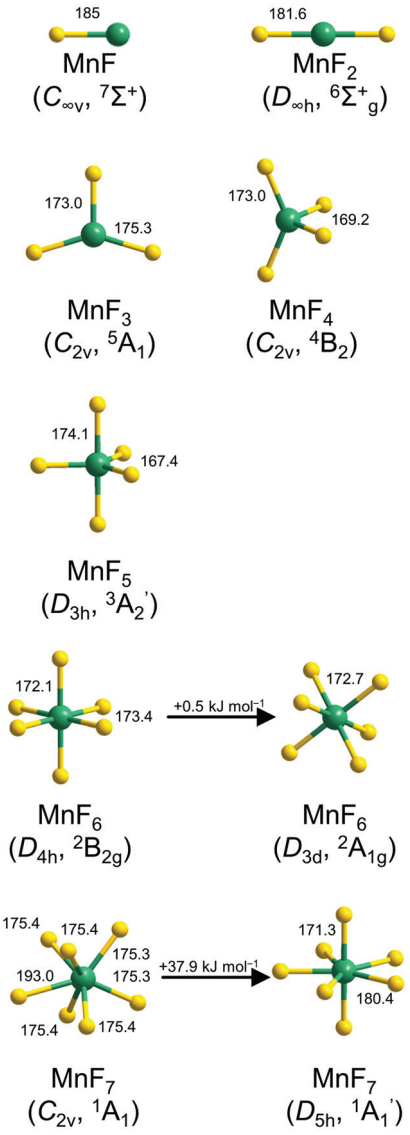

Fig. 1 Optimized structures of molecular manganese fluorides at the CCSD(T) ($MnF–MnF_5$) and DFT levels (MnF_6 and MnF_7). Selected bond lengths (pm) and angles (°) are indicated. For a complete list see also Table S1 in the ESI.‡

The quintet ground state shows two longer Mn–F bonds (175.3 pm) and one shorter Mn–F bond (173.0 pm) at the CCSD(T) level, which is in very good agreement with the results from gas phase electron diffraction (175.4 pm and 172.8 pm).[16] According to our CCSD(T) calculations MnF_4 has a distorted tetrahedral structure (C_{2v} symmetry) with Mn–F bond lengths of 173.0 pm and 169.2 pm. For MnF_5 a trigonal bipyramidal minimum structure (D_{3h} symmetry) with bond lengths of 174.1 pm ($Mn–F_{ax}$) and 167.4 pm ($Mn–F_{eq}$) was computed at the CCSD(T) level. The d^1 electron configuration of manganese in MnF_6 causes a distortion from a regular octahedral structure which leads to either a structure with D_{4h}- or D_{3d}-symmetry. Both isomers are minima on the potential energy surface with the trigonal antiprismatic structure (bond lengths of 172.7 pm) just 0.5 kJ mol^{-1} in energy above the tetragonal bipyramidal structure ($Mn–F_{ax}$ 172.1 pm, $Mn–F_{eq}$ 173.4 pm) at the CCSD(T)/aug-cc-pVTZ//B3LYP/aug-cc-pVTZ level. For MnF_7 also two minimum structures were computed at the DFT level. The regular D_{5h}-symmetrical pentagonal bipyramidal isomer exhibits $Mn–F_{ax}$ bond lengths of 171.3 pm and $Mn–F_{eq}$ bond lengths of 180.4 pm. The monocapped trigonal prismatic isomer revealed four Mn–F bonds of 175.4 pm and two slightly shorter bonds of 175.3 pm, while the seventh fluorine atom is considerably weaker bound with 193.0 pm (Fig. 1). At the CCSD(T)/aug-cc-pVTZ//B3LYP/aug-cc-pVTZ level the latter isomer is favored in energy by 37.9 kJ mol^{-1}. This is in contrast to the computed minimum structure of TcF_7 [31] and the crystal structure of ReF_7 [37] which both are (slightly) distorted pentagonal bipyramids. The reason for this disparity could be the smaller radius of the manganese atom compared to technetium and rhenium atoms.

The observability of a transient molecule in a matrix-isolation experiment requires at least a marginal thermochemical stability. This can be assessed by calculating the enthalpy of possible decomposition reactions. Table 1 lists the corres-

Table 1 Calculated decomposition enthalpies at 0 K, ΔH (0 K) = ΔE + ΔZPE, of molecular manganese fluorides[a]

	B3LYP		CCSD(T)	
Reaction	ΔE	ΔE + ΔZPE	ΔE	ΔE + ΔZPE
$MnF_7 \rightarrow MnF_5 + F_2$	−394.5	−399.9	−357.5[b]	—
$MnF_7 \rightarrow MnF_6 + \frac{1}{2}F_2$	−271.7	−275.6	−195.3[b]	—
$MnF_7 \rightarrow MnF_6 + F$	−194.1	−201.1	−119.3[b]	—
$MnF_6 \rightarrow MnF_4 + F_2$	−67.9	−76.5	−141.5[b]	—
$MnF_6 \rightarrow MnF_5 + \frac{1}{2}F_2$	−122.8	−124.3	−162.2[b]	—
$MnF_6 \rightarrow MnF_5 + F$	−45.2	−49.8	−86.6[b]	—
$MnF_5 \rightarrow MnF_3 + F_2$	217.4	206.5	131.7	119.9
$MnF_5 \rightarrow MnF_4 + \frac{1}{2}F_2$	54.9	47.7	20.2	12.9
$MnF_5 \rightarrow MnF_4 + F$	132.5	122.2	96.5	86.4
$MnF_4 \rightarrow MnF_2 + F_2$	405.0	397.8	304.1	295.3
$MnF_4 \rightarrow MnF_3 + \frac{1}{2}F_2$	162.5	158.7	111.4	107.0
$MnF_4 \rightarrow MnF_3 + F$	240.1	233.2	187.7	180.5
$MnF_3 \rightarrow MnF_2 + \frac{1}{2}F_2$	242.6	239.1	192.6	188.3
$MnF_3 \rightarrow MnF_2 + F$	320.2	313.6	268.9	261.8

[a] Values in kJ mol^{-1}. [b] CCSD(T)/aug-cc-pVTZ//B3LYP/aug-cc-pVTZ.

Table 2 Calculated and experimentally observed IR wavenumbers of Mn–F stretching modes of molecular manganese fluorides[a]

		Calc.				Exp.		
Molecule	Mode	B3LYP		CCSD(T)		Ne	Ar	N_2
MnF ($C_{\infty v}$, $^7\Sigma^+$)	Σ^+	607.7	(134)	605.9[b]	—	608.5[c]	589.2[c] *588.6*[d]	585.8[c]
MnF_2 ($D_{\infty h}$, $^6\Sigma^+_g$)	Σ^-_u	723.5	(237)	721.3	(209)	721.6[c] *722.1*[e]	699.6[c] *700.1*[e] *699*[d] *699.5*[f]	
MnF_3 (C_{2v}, $^5A_1$)	A_1	646.1	(9)	656.7	(15)	657.1[c]	643.7[c] *644*[g]	
	A_1	720.9	(126)	729.9	(134)	726.9[c] *728*[g]	711.2[c] *712*[g] *711*[d] *711.2*[f]	
	B_2	764.2	(256)	779.3	(287)	773.4[c] *774*[g]	758.7[c] *759*[g] *758*[d] *758.5*[f]	
MnF_4 (C_{2v}, $^4B_2$)	A_1	675.0	(18)	681.5	(13)			
	A_1	749.3	(85)	755.5	(83)			
	B_1	752.3	(261)	777.9	(299)		*768.7*[d]	
	B_2	792.8	(123)	800.0	(105)		*794.5*[f]	
MnF_5 (D_{3h}, $^3A'_2$)	A''_2	742.7	(299)	768.5	(331)			
	E'	816.9	(272)	824.4	(235)			

[a] Values in cm^{-1}, IR intensities in km mol^{-1} in parentheses. [b] Ref. 6. [c] This work. [d] Ref. 11. [e] Ref. 20. [f] Ref. 23. [g] Ref. 21.

ponding reaction enthalpies for the optimized manganese fluorides.

The decomposition of MnF_7 and MnF_6 is strongly exothermic at all considered pathways including concerted elimination of F_2, bimolecular reaction and homolytic bond fission. For MnF_5 however the decomposition channels are computed to be endothermic at the CCSD(T) level. Thus, it should be possible to obtain molecular MnF_5 under appropriate conditions, for example in matrix-isolation experiments. However, ΔG (298.15 K) for the gas phase reaction $MnF_5 \rightarrow MnF_4 + \frac{1}{2}F_2$ is calculated to be −12.2 kJ mol^{-1} at the CCSD(T)/aug-cc-pVTZ level, so molecular MnF_5 is not stable at ambient temperatures in the gas phase. Considering that sublimation enthalpies are usually smaller for the higher fluorides, MnF_5 is most likely also not stable in the condensed phase. The value of ΔH(0 K) = 107.0 kJ mol^{-1} obtained for the decomposition $MnF_4 \rightarrow MnF_3 + \frac{1}{2}F_2$ also suggests a low thermal stability of molecular MnF_4, which is consistent with the reported vapor pressure of F_2 over solid MnF_4 at room temperature.[29]

Vibrational spectra of the manganese fluorides were calculated at the DFT ($MnF–MnF_7$) and CCSD(T) levels ($MnF–MnF_5$). The corresponding Mn–F stretching wavenumbers for $MnF–MnF_5$ are listed and compared to experimentally observed IR bands in Table 2. Calculated IR wavenumbers of Mn–F stretching modes for MnF_6 and MnF_7 are listed in Table S2.‡

Matrix-isolation experiments

Molecular manganese fluorides were generated by IR-laser (λ = 1064 nm) ablation of a rotating elemental manganese target and co-condensed with fluorine diluted (0.25–3%) in neon or argon. After deposition of the sample new IR absorptions in the Mn–F stretching region were observed. Fig. 2 shows spectra obtained after deposition of the reaction products of manganese atoms with varying concentrations of F_2 in Ar. The most intense band obtained with fluorine concentrations up to 1%, observed at 699.6 cm^{-1} in Ar and 721.6 cm^{-1} in Ne,

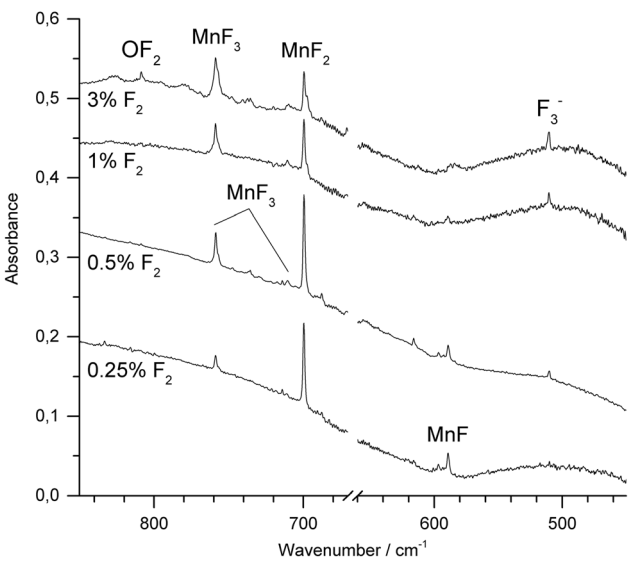

Fig. 2 IR spectra in the 450–850 cm^{-1} region of the Ar matrix-isolated (12 K) reaction products of laser ablated manganese atoms in the presence of F_2 (0.25–3%) after 1 h of deposition. The region of the bending mode of atmospheric CO_2 (660–670 cm^{-1}) was omitted for a better representation.

respectively (ESI; Fig. S1‡), is associated with the Σ^-_u-mode of MnF_2. Bands of MnF_3 were observed at 758.7 cm^{-1} and 711.2 cm^{-1} in Ar and at 773.4 cm^{-1} and 726.9 cm^{-1} in Ne, respectively. These values agree very well with those from experiments of thermally evaporated manganese difluoride and trifluoride, respectively.[20,21] While the intensity of the band due to MnF_2 increased going from 0.25% to 0.5% F_2 and then decreased with higher fluorine content, the intensity of the bands due to MnF_3 increased steadily. Also the antisymmetric stretching band of $[F_3]^-$ has been observed at 510.1 cm^{-1}. This anion has been shown to be formed from F^- and a F_2 molecule during the deposition process, where the F^- anion arises from a fluorine atom by electron capture in the plasma plum of an IR-laser ablated metal.[38,39] A decrease in intensity with increasing fluorine concentration was observed for the band at 589.2 cm^{-1}, which is assigned to diatomic MnF, which is in excellent agreement with a previous report.[11] Its counterpart in Ne was observed at 608.5 cm^{-1} (ESI; Fig. S1‡). This wavenumber is consistent with an estimated value of 612.0 cm^{-1} obtained by rotational spectroscopy[40] considering the red-shift of transition metal monofluoride bands experienced in solid noble gases.[41] To the best of our knowledge this is the first report about MnF isolated in a neon matrix. It is noteworthy that IR-laser ablation of elemental manganese in the presence of fluorine did not produce any higher fluoride than MnF_3. Irradiation of Ar-isolated F_2 molecules with λ = 455 ± 10 nm is proved to produce reactive F-atoms, which are subject to a restricted movement within the solid Ar matrix, and thus may react with adjacent molecules such as MnF_3. However, even this photolysis of the deposit failed to produce higher fluorides of manganese.

When neat fluorine was used as matrix gas, several metal dependent absorptions could also be observed within Mn-F stretching range between 730 cm^{-1} and 780 cm^{-1} (ESI; Fig. S2‡). However, these absorptions were broad and relatively weak in intensity, and their assignment appeared to be difficult. Band broadening and overlapping features were also observed using N_2 or 1% F_2 in N_2 together with IR-laser ablated manganese atoms (ESI; Fig. S3‡). This result is most likely due to the presence of several matrix sites. However, based on its behavior upon annealing and photolysis a band at 585.8 cm^{-1} in solid N_2 could be unambiguously assigned to molecular MnF.

We have also conducted IR-laser ablation experiments using a pressed target pellet made of MnF_3. Very recently we reported about the laser ablation of alkali metal fluorides,[42] but, to the best of our knowledge, IR-laser ablation of solid transition metal fluorides has not yet been explored. Molecular MnF_3 generated from a solid MnF_3 target was first co-condensed with an excess of Ne at 5 K (Fig. 3) and produced bands at 773.4 cm^{-1} and 726.9 cm^{-1}. The presence of MnF_2 (Σ^-_u: 721.6 cm^{-1}) indicates some decomposition of MnF_3 in the plasma plum, probably by F-atom elimination.

When Ar was used as matrix gas (Fig. 4), the band for MnF_2 shifts to 699.6 cm^{-1} and those of MnF_3 to 758.7 cm^{-1} and 711.2 cm^{-1}. Additionally, the weaker third Mn–F stretching

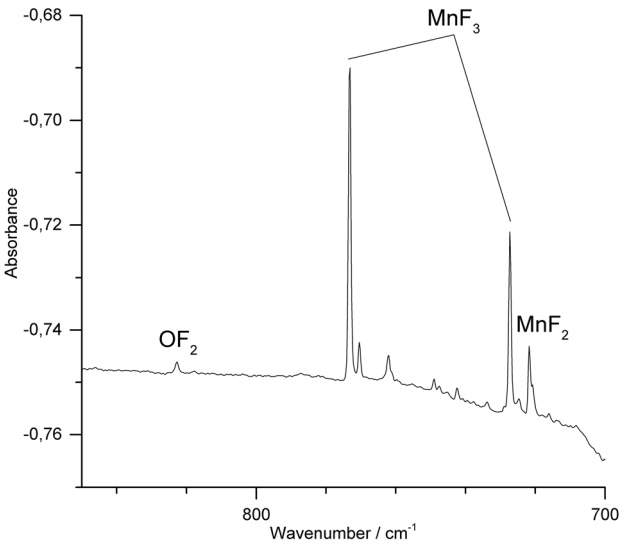

Fig. 3 IR spectrum in the 700–850 cm^{-1} region of the Ne matrix-isolated (5 K) products of laser ablated solid MnF_3 after 15 min of deposition.

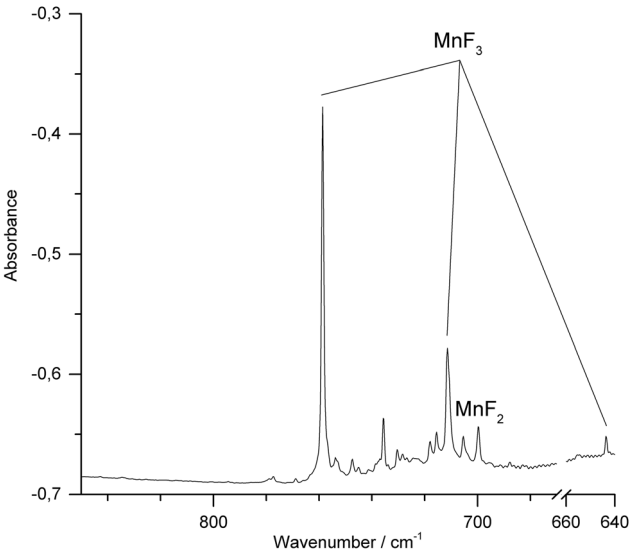

Fig. 4 IR spectrum in the 640–850 cm^{-1} region of Ar matrix-isolated (12 K) products of laser ablated solid MnF_3 after 15 min of deposition. The region of the bending mode of atmospheric CO_2 (660–670 cm^{-1}) was omitted for a better representation.

band of MnF_3 was observed at 643.7 cm^{-1}. A sharp band observed at 735.7 cm^{-1} could not be assigned to a mononuclear MnF_2 or MnF_3 species. This band was previously also observed by the thermal evaporation of solid MnF_3 and tentatively assigned to a fluorine bridged dimer.[11] In addition, traces of oxygen containing species such as OF_2 and MnO_3F[43–45] were detected (ESI; Fig. S4 and S5‡). Although the target was prepared and fixed to the target holder under inert conditions, some superficial hydrolysis could probably not be

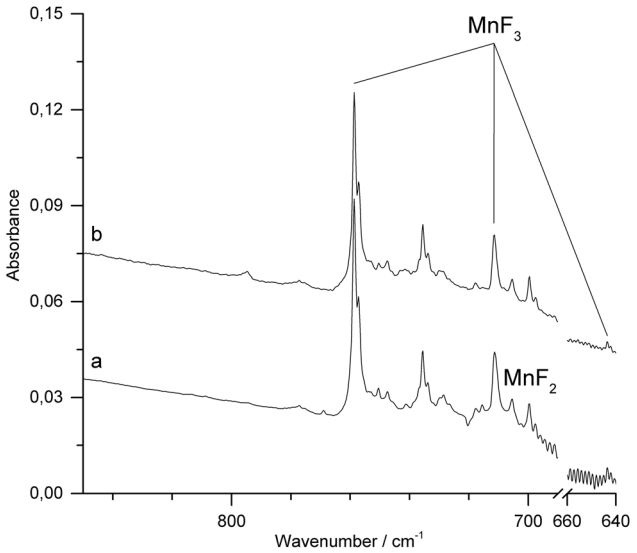

Fig. 5 IR spectra in the 640–850 cm^{-1} region of Ar matrix-isolated (12 K) products of laser ablated solid MnF_3 in the presence of F_2 (1%). (a) After 15 min of deposition. (b) After 15 min of λ = 455 ± 10 nm irradiation. The region of the bending mode of atmospheric CO_2 (660–670 cm^{-1}) was omitted for a better representation.

prevented during the preparation of the target. The oxygen species OF_2 and MnO_3F might then have been formed in the plasma plum from the products of this hydrolysis.

IR-laser ablation of solid MnF_3 was also carried out in the presence of fluorine (1% F_2 in Ar). Apart from some line broadening, the spectrum (Fig. 5a and ESI; Fig. S6‡) is very similar to that obtained without fluorine (Fig. 4). After photolysis (λ = 455 ± 10 nm) a weak feature at 795 cm^{-1} appeared, which did not grow further with prolonged photolysis (Fig. 5b).

The carrier of this weak band is difficult to assign. A single IR band in the Mn–F stretching region at 794.5 cm^{-1} was previously obtained in solid Ar from the vaporization of a mixture of MnF_3 and TbF_4 at 700 K and assigned to molecular MnF_4.[23] From their observation, the authors inferred a tetrahedral structure of molecular MnF_4. However, the presence of a single Mn–F stretching band is not in agreement with the calculated C_{2v} structure of MnF_4 (Fig. 1), for which at least three strong Mn–F stretching bands are predicted (Table 2). The previous assignment of molecular MnF_4 to a single Mn–F stretching band at 794.5 cm^{-1} is therefore questionable, and the carrier of the strong IR band obtained in these experiments remains unknown.

Experimental and theoretical methods

Matrix-isolation experiments

CAUTION: Appropriate safety precautions should be taken into account when handling pure fluorine and metal fluorides. All equipment has to be adequately pretreated with fluorine prior to use. Note that sudden freezing of samples in metal cylinders to liquid nitrogen temperatures is potentially dangerous. The suitability of metal cylinders for such a cooling procedure should be proven and the cylinders should always be leak tested at liquid nitrogen temperature prior to filling with poisonous samples. The setup for matrix-isolation and IR-laser ablation experiments has been described in detail previously.[35] The 1064 nm fundamental of a Nd:YAG laser was focused onto a freshly sanded rotating manganese (chemPUR, 99.99%) target or target pellets made of MnF_3 (Alfa Aesar, 98%). Gaseous mixtures of various concentrations (0.25–100%) of fluorine (Solvay Fluor AG, 99.998%) in neon (Air Liquide, 99.999%), argon (SWF, 99.999%) and nitrogen (Linde, 99.999%) were prepared using a fluorine cylinder (V = 1000 cm^3, thick-walled stainless steel, $p_{298\ K} < 1$ bar) cooled to 77 K to freeze out less volatile impurities such as traces of HF and CO_2. These mixtures were than co-condensed together with the IR-laser ablated species for 45–60 min onto a CsI cold window cooled to 5 K (Ne matrices) or 12 K (Ar and F_2). Pure fluorine matrices were deposited onto a protective layer of argon to prevent oxidation of the cold window material. FTIR spectra were recorded at a resolution of 0.5 cm^{-1} on a Bruker Vertex 70 spectrometer equipped with a KBr beam splitter using a liquid nitrogen cooled mercury cadmium telluride (LN-MCTB) detector. A common IR band observed in all spectra of such experiments using IR-laser ablated metal atoms and fluorine is due to the $[F_3]^-$ anion at 510.1 cm^{-1} (Ar), 517.2 cm^{-1} (N_2), or 524.6 cm^{-1} (Ne), respectively.[46] As no isotopic splitting of the IR bands of both the monoisotopic manganese and fluorine elements can be observed, any assignment of bands of binary manganese and fluorine species mainly relies on reliably calculated spectra and meaningful variations of experimental conditions.

Quantum-chemical calculations

Structures of the manganese fluorides MnF_x (x = 1–7) displayed in Fig. 1 were fully optimized at the DFT level using the B3LYP functional[47–49] in conjunction with the aug-cc-pVTZ basis sets for fluorine[50] and manganese,[51] and considering all reasonable spin multiplicities. Subsequent optimizations at the CCSD(T) level were carried out for the ground states of MnF_x (x = 2–5). Harmonic frequencies were calculated for stationary points on the potential energy surface. The DFT calculations were performed with Gaussian09[52] and CFOUR[53] was used for the coupled-cluster calculations.

Conclusion

For more than 50 years solid MnF_4 has been the highest experimentally known manganese fluoride, but experimental data about its molecular structure are still missing. Quantum-chemical calculations at the CCSD(T) level predict molecular MnF_4 to be stable against its decomposition according to $MnF_4 \rightarrow MnF_3 + \frac{1}{2}F_2$ by ΔH(0 K) = 107 kJ mol^{-1}. The corresponding decomposition route for the unprecedented MnF_5 ($MnF_5 \rightarrow MnF_4 + \frac{1}{2}F_2$) is found to be only marginally endother-

mic by $\Delta H(0\ \mathrm{K}) = 12.9\ \mathrm{kJ\ mol^{-1}}$. Molecular MnF_6 and MnF_7 are unstable with respect to their decomposition to lower manganese fluorides. The reaction of IR-laser ablated manganese atoms with elemental fluorine diluted in neon, argon and nitrogen and neat fluorine was studied. The IR analysis of the matrix-isolated products at 5–12 K revealed the formation of molecular MnF, MnF_2 and MnF_3. Molecular MnF_3 has alternatively been produced and matrix-isolated by IR-laser ablation of a solid manganese trifluoride target. Attempts to detect IR bands of a higher manganese fluoride such as MnF_4 or MnF_5 by carrying out these experiments in the presence of elemental fluorine or by additional UV photolysis of the deposits failed. The presented results cast doubt on previous reports about the formation of such higher molecular manganese fluorides either from the reaction between MnF_3 and TbF_4[23] or by thermal evaporation of Mn atoms in the presence of fluorine.[11]

Acknowledgements

The authors thank the Fonds der Chemischen Industrie and the Deutsche Forschungsgemeinschaft (HA 5639/3-1 and GRK 1582/2 "Fluorine as a Key Element") for financial support.

References

1 S. Mukhopadhyay, S. K. Mandal, S. Bhaduri and W. H. Armstrong, *Chem. Rev.*, 2004, **104**, 3981–4026.
2 F. Margueritte, *C. R. Acad. Sci.*, 1846, **100**, 380–385.
3 W. Zhang and C. Y. Cheng, *Hydrometallurgy*, 2007, **89**, 137–159.
4 H. Aschoff, *Ann. Phys. Chem.*, 1860, **2**(111), 217–229.
5 S. Riedel and M. Kaupp, *Coord. Chem. Rev.*, 2009, **253**, 606–624.
6 P. V. Nhat, N. T. Cuong, P. K. Duy and M. T. Nguyen, *Chem. Phys.*, 2012, **400**, 185–197.
7 R. A. Kent, T. C. Ehlert and J. L. Margrave, *J. Am. Chem. Soc.*, 1964, **86**, 5090–5093.
8 O. Launila and B. Simard, *J. Mol. Spectrosc.*, 1992, **154**, 93–118.
9 O. Launila, B. Simard and A. M. James, *J. Mol. Spectrosc.*, 1993, **159**, 161–174.
10 P. M. Sheridan and L. M. Ziurys, *Chem. Phys. Lett.*, 2003, **380**, 632–646.
11 S. B. Osin, D. I. Davlyatshin, V. F. Shevelkov and V. N. Mitkin, *Russ. J. Phys. Chem.*, 1995, **69**, 794–799.
12 T. C. DeVore, R. J. Van Zee and W. Weltner Jr., *J. Chem. Phys.*, 1978, **68**, 3522–3527.
13 R. J. Van Zee, C. M. Brown and W. Weltner Jr., *Chem. Phys. Lett.*, 1979, **64**, 325–328.
14 P. Mondal, D. Opalka, L. V. Poluyanov and W. Domcke, *Chem. Phys.*, 2011, **387**, 56–65.
15 N. Vogt, *J. Mol. Struct.*, 2001, **570**, 189–195.
16 M. Hargittai, B. Réffy, M. Kolonits, C. J. Marsden and J.-L. Heully, *J. Am. Chem. Soc.*, 1997, **119**, 9042–9048.
17 M. A. Hepworth and K. H. Jack, *Acta Crystallogr.*, 1957, **10**, 345–351.
18 J. V. Rau, V. Rossi Albertini, N. S. Chilingarov, S. Colonna and U. Anselmi Tamburini, *J. Fluorine Chem.*, 2001, **108**, 253–256.
19 Z. Yamani, Z. Tun and D. H. Ryan, *Can. J. Phys.*, 2010, **88**, 771–797.
20 J. W. Hastie, R. Hauge and J. L. Margrave, *J. Chem. Soc. D*, 1969, 1452–1453.
21 V. N. Bukhmarina and Y. B. Predtechenskii, *Opt. Spectrosc.*, 1996, **80**, 684–687.
22 Z. Mazej, *J. Fluorine Chem.*, 2002, **114**, 75–80.
23 S. N. Cesaro, J. V. Rau, N. S. Chilingarov, G. Balducci and L. N. Sidorov, *Inorg. Chem.*, 2001, **40**, 179–181.
24 R. Hoppe, W. Dähne and W. Klemm, *Naturwissenschaften*, 1961, **11**, 429.
25 K. O. Christe, *Inorg. Chem.*, 1986, **25**, 3721–3722.
26 B. G. Müller and M. Serafin, *Z. Naturforsch.*, 1987, **42b**, 1102–1106.
27 M. Adelhelm and E. Jacob, *J. Fluorine Chem.*, 1991, **54**, 21.
28 K. Lutar, A. Jesih and B. Zemva, *Polyhedron*, 1988, **7**, 1217–1219.
29 R. Hoppe, W. Dähne and W. Klemm, *Justus Liebigs Ann. Chem.*, 1962, **658**, 1–5.
30 H. Selig, C. L. Chernick and J. G. Malm, *J. Inorg. Nucl. Chem.*, 1961, **19**, 377.
31 S. Riedel, M. Renz and M. Kaupp, *Inorg. Chem.*, 2007, **46**, 5734–5738.
32 J. G. Malm, H. Selig and S. Fried, *J. Am. Chem. Soc.*, 1960, **82**, 1510.
33 T. Schlöder, T. Vent-Schmidt and S. Riedel, *Angew. Chem., Int. Ed.*, 2012, **51**, 12063–12067, (*Angew. Chem.*, 2012, **124**, 12229–12233).
34 A. J. Edwards, *Proc. Chem. Soc., London*, 1963, 205.
35 T. Schlöder, F. Brosi, B. J. Freyh, T. Vent-Schmidt and S. Riedel, *Inorg. Chem.*, 2014, **53**, 5820–5829.
36 M. I. Nikitin and E. G. Rakov, *Russ. J. Inorg. Chem.*, 1998, **43**, 314–318.
37 T. Vogt, A. N. Fitch and J. K. Cockcroft, *Science*, 1994, **263**, 1265–1267.
38 T. Vent-Schmidt, F. Brosi, J. Metzger, T. Schlöder, X. Wang, L. Andrews, C. Müller, H. Beckers and S. Riedel, *Angew. Chem., Int. Ed.*, 2015, **54**, 8279–8283, (*Angew. Chem.*, 2015, **127**, 8397–8401).
39 F. Brosi, T. Vent-Schmidt, S. Kieninger, T. Schlöder, H. Beckers and S. Riedel, *Chem. – Eur. J.*, 2015, **21**, 16455–16462.
40 G. D. Rochester and E. Olsson, *Z. Phys.*, 1939, **114**, 495–499.
41 X. Wang, L. Andrews, F. Brosi and S. Riedel, *Chem. – Eur. J.*, 2013, **19**, 1397–1409.
42 F. A. Redeker, H. Beckers and S. Riedel, *RSC Adv.*, 2015, **5**, 106568–106573.

43 P. J. Aymonino, H. Schulze and A. Müller, *Z. Naturforsch., B: Anorg. Chem. Org. Chem. Biochem. Biophys. Biol.*, 1969, **24**, 1508–1510.
44 M. J. Reisfeld, L. B. Asprey and N. A. Matwiyoff, *Spectrochim. Acta*, 1970, **27**, 765–772.
45 E. L. Varetti and A. Müller, *Z. Anorg. Allg. Chem.*, 1978, **442**, 230–234.
46 S. Riedel, T. Köchner, X. Wang and L. Andrews, *Inorg. Chem.*, 2010, **49**, 7156–7164.
47 A. D. Becke, *J. Chem. Phys.*, 1993, **98**, 5648–5652.
48 C. Lee, Y. Yang and R. G. Parr, *Phys. Rev. B: Condens. Matter*, 1988, **37**, 785–789.
49 B. Miehlich, A. Savin, H. Stoll and H. Preuss, *Chem. Phys. Lett.*, 1989, **157**, 200–206.
50 R. A. Kendall, T. H. Dunning Jr. and R. J. Harrison, *J. Chem. Phys.*, 1992, **96**, 6796–6806.
51 N. B. Balabanov and K. A. Peterson, *J. Chem. Phys.*, 2005, **123**, 064107.
52 M. J. Frisch, G. W. Trucks, H. B. Schlegel, G. E. Scuseria, M. A. Robb, J. R. Cheeseman, G. Scalmani, V. Barone, B. Mennucci, G. A. Petersson, H. Nakatsuji, M. Caricato, X. Li, H. P. Hratchian, A. F. Izmaylov, J. Bloino, G. Zheng, J. L. Sonnenberg, M. Hada, M. Ehara, K. Toyota, R. Fukuda, J. Hasegawa, M. Ishida, T. Nakajima, Y. Honda, O. Kitao, H. Nakai, T. Vreven, J. A. Montgomery Jr., J. E. Peralta, F. Ogliaro, M. Bearpark, J. J. Heyd, E. Brothers, K. N. Kudin, V. N. Staroverov, R. Kobayashi, J. Normand, K. Raghavachari, A. Rendell, J. C. Burant, S. S. Iyengar, J. Tomasi, M. Cossi, N. Rega, N. J. Millam, M. Klene, J. E. Knox, J. B. Cross, V. Bakken, C. Adamo, J. Jaramillo, R. Gomperts, R. E. Stratmann, O. Yazyev, A. J. Austin, R. Cammi, C. Pomelli, J. W. Ochterski, R. L. Martin, K. Morokuma, V. G. Zakrzewski, G. A. Voth, P. Salvador, J. J. Dannenberg, S. Dapprich, A. D. Daniels, Ö. Farkas, J. B. Foresman, J. V. Ortiz, J. Cioslowski and D. J. Fox, *Gaussian 09, Revision B.01*, Gaussian, Inc., Wallingford CT, 2009.
53 CFOUR, Coupled-Cluster techniques for Computational Chemistry, a quantum-chemical program package by J. F. Stanton, J. Gauss, M. E. Harding, P. G. Szalay with contributions from A. A. Auer, R. J. Bartlett, U. Benedikt, C. Berger, D. E. Bernholdt, Y. J. Bomble, L. Cheng, O. Christiansen, M. Heckert, O. Heun, C. Huber, T.-C. Jagau, D. Jonsson, J. Jusélius, K. Klein, W. J. Lauderdale, D. A. Matthews, T. Metzroth, L. A. Mück, D. P. O'Neill, D. R. Price, E. Prochnow, C. Puzzarini, K. Ruud, F. Schiffmann, W. Schwalbach, C. Simmons, S. Stopkowicz, A. Tajti, J. Vázquez, F. Wang and J. D. Watts and the integral packages *MOLECULE* (J. Almlöf and P. R. Taylor), *PROPS* (P. R. Taylor), *ABACUS* (T. Helgaker, H. J. Aa. Jensen, P. Jørgensen, and J. Olsen), and ECP routines by A. V. Mitin and C. van Wüllen. For the current version, see http://www.cfour.de.